

# Short-range dynamics of a nematic liquid-crystalline phase

Andreas S. Poulos,<sup>1</sup> Doru Constantin,<sup>1, a)</sup> Patrick Davidson,<sup>1</sup> Brigitte Pansu,<sup>1</sup> Éric Freyssingeas,<sup>2</sup> Anders Madsen,<sup>3</sup> and Corinne Chanéac<sup>4</sup>

<sup>1)</sup> *Laboratoire de Physique des Solides, Université Paris-Sud, CNRS, UMR 8502, 91405 Orsay, France.*

<sup>2)</sup> *Laboratoire de Physique, École Normale Supérieure de Lyon, CNRS, UMR 5672, 69364 Lyon, France.*

<sup>3)</sup> *European Synchrotron Radiation Facility, Boîte Postale 220, 38043 Grenoble, France.*

<sup>4)</sup> *Laboratoire de Chimie de la Matière Condensée, Université Paris 6, CNRS, UMR 7574, 75252 Paris, France.*

(Dated: 13 September 2021)

Using X-ray photon correlation spectroscopy, we studied the dynamics in the nematic phase of a nanorod suspension. The collective diffusion coefficient in the plane perpendicular to the director varies sharply with the wave vector. Combining the structure factor and the diffusion coefficient we find that the hydrodynamic function of the phase decreases by more than a factor of ten when going from length scales comparable to the inter-particle distance towards larger values. Thus, the collective dynamics of the nematic phase experiences strong and scale-dependent slowing down, in contrast with isotropic suspensions of slender rods or of spherical particles.

PACS numbers: 82.70.Dd, 87.15.Ya, 61.05.cf

Keywords: colloid; nematic; hydrodynamics; X-ray

Nematics are the simplest example of a phase with no positional order, but still exhibiting orientational order (and hence anisotropy). This combination endows them with remarkable qualities: although fluid, they have elastic properties and, consequently, long-lived fluctuations. A great deal is known about the large-scale behaviour of nematic systems, which is well-described by a generalized hydrodynamic model<sup>1</sup>. This theoretical description was confirmed (and refined) using a wealth of experimental techniques. The method of choice for studying nematodynamics is dynamic light scattering (DLS), which is sensitive to the relaxation of nematic fluctuations on micron scales<sup>2,3</sup>.

On the other hand, there is much less data on the short-range dynamics of the nematic phase, converging length scales comparable to the inter-particle distance. In this limit, the continuous medium model is bound to break down, and more microscopic considerations must be taken into account. Since this is the scale at which interaction between particles defines the structure of the system, understanding the dynamics is essential for building a complete picture of the phase. A considerable body of theoretical and numerical work exists<sup>4,5</sup>, but there is very little experimental data, mainly due to the lack of adapted techniques (due to the typical particle size, this range of scattering vectors is out of reach for DLS.) Alternative methods can be used, such as inelastic neutron scattering, which is however limited to sub-microsecond dynamics (too fast for cooperative processes). Spin relaxation has also been employed, but it

lacks the required space resolution and the conclusions are indirect.

X-ray scattering techniques are suitable for exploring these distances, but until recently they were only able to draw a *static* picture of the system. This situation is changing due to the progress of X-ray photon correlation spectroscopy (XPCS), opening up the time dimension. However, due to inherent technical difficulties, the experimental systems must fulfill very stringent conditions, such as slow relaxation rates and high scattering contrast. Some experiments have already been performed on nematics using XPCS, but they were only concerned with very slow relaxation in a gel phase<sup>6</sup> or with capillary surface waves<sup>7</sup>.

Essential information on the physics of multi-particle systems is contained in the structure factor  $S(q)$  and the collective diffusion coefficient  $D(q)$ <sup>8</sup>. Based on very general thermodynamic arguments, these parameters are related by  $D(q) \sim 1/S(q)$  (“de Gennes narrowing”<sup>9</sup>). In colloidal suspensions, a more refined treatment must take into account the hydrodynamic interactions, which further modulate this dependence.

In this letter, we study a fluid nematic phase of goethite ( $\alpha$ -FeOOH) nanorods (with moderate aspect ratio) and determine the hydrodynamic function over a  $q$ -range corresponding to length scales comparable to the inter-particle distances. Unexpectedly, we find that for wave vectors  $q < q_{\max}$  (below the maximum of the structure factor), the dynamics of the system slows down considerably. This result is in stark contrast with isotropic suspensions of slender rods, where no hydrodynamic effect is observed<sup>10</sup>. Furthermore, the effect is much stronger than the variation of the hydrodynamic function in suspensions of colloidal spheres<sup>11</sup>, emphasizing

<sup>a)</sup> Electronic mail: constantin@lps.u-psud.fr

the role of particle anisotropy and of the nematic order.

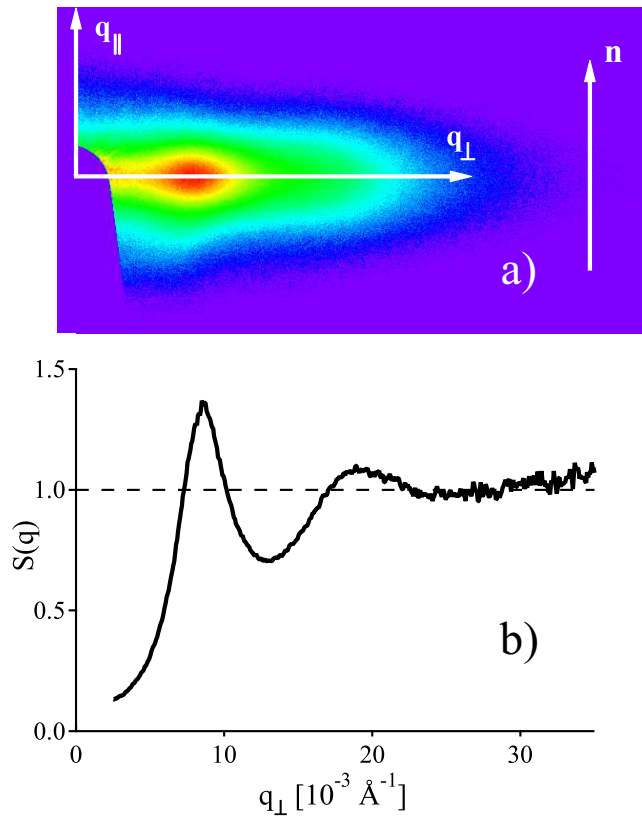


FIG. 1. a) SAXS pattern of an aligned nematic sample with  $\phi_g = 6.7\%$  at 228 K. The arrow indicates the direction of the nematic director  $\vec{n}$ . b) Structure factor along the  $q_\perp$  direction calculated from the SAXS data in a).

Goethite nanoparticles were synthesized according to a well-established procedure and dispersed in water<sup>12,13</sup>. The particles are lath-shaped; transmission electron microscopy images show that they are  $4000 \pm 1000$  Å long and  $330 \pm 110$  Å wide (mean and standard deviation obtained from a log-normal fit). Moreover, the particle cross-section is usually anisotropic by a factor of 2.5<sup>13</sup>. In the following, we therefore consider that the particles rotate freely around their main axis, as expected in a uniaxial nematic phase. In order to slow down their dynamics so that it may be conveniently studied by XPCS, the particles were resuspended in an 80 wt.% propane-1,3-diol in water mixture. Although this mixture has lower dielectric permittivity than water, the particles still bear some positive electrical surface charge density, which ensures the colloidal stability of the suspension. In the first approximation, the effect of electrostatic interactions can be described by introducing an effective radius larger than the bare one, which tends to reduce the apparent particle aspect ratio<sup>14</sup>. For example, previous studies of another goethite suspension in pure water have shown that the ratio of effective diameter to bare diameter is about 1.6<sup>15</sup>. With the solvent mixture used here, this electrostatic correction factor is expected to be smaller.

Therefore, in the following, the particles will be considered as cylindrical rods, 4000 Å long and with an aspect ratio of about 10. (The interpretation presented below does not critically depend on the precise value of the effective aspect ratio.) At volume fractions  $\phi_g \leq 4.2\%$  the suspensions are isotropic, whereas at  $\phi_g \geq 6.7\%$  they form a nematic liquid-crystalline phase that aligns in low magnetic field, with its nematic director parallel to the field<sup>16</sup>. Samples of different volume fractions were held in optical flat glass capillaries, 50 μm thick (VitroCom, NJ, USA) and placed in a vacuum chamber. The temperature was lowered to 228 K, where the viscosity of the solvent is of the order of 1000 mPa.s. The nematic phase was aligned with a 150 mT field that was then removed for the actual measurements.

The small-angle X-ray scattering (SAXS) and XPCS measurements were performed at the TROIKA beam line ID10A of the ESRF with an X-ray energy of 8 keV ( $\lambda = 1.55$  Å) selected by a single-bounce Si(111) monochromator, in the uniform filling mode of the storage ring. A (partially) coherent beam is obtained by inserting a 10 μm pinhole aperture a few centimetres upstream of the sample.

For the XPCS measurements, we used a two-dimensional (2D) Maxipix detector consisting of  $256 \times 256$  square pixels (55 μm in size), and the intensity autocorrelation functions were calculated by ensemble averaging over equivalent pixels<sup>17</sup>. In the nematic phase, the pixels averaged were restricted to a narrow slice perpendicular to the nematic director for  $q_\perp$  (see Figure 1 for an illustration and Figure 2 for the results), or parallel to the nematic director for  $q_\parallel$ . In the isotropic phase, all pixels at the same scattering vector modulus were averaged. Some measurements were also performed using a point detector (an avalanche photodiode) connected to an external digital correlator (Flex01D-08).

A typical SAXS pattern of an aligned nematic sample is shown in Figure 1a. The static structure factor  $S(q_\perp)$  in the  $q_\perp$  direction (Figure 1b) was obtained by dividing the scattered intensity by the form factor measured independently on a dilute solution.  $S(q_\perp)$  displays a well-defined interaction peak, at a value  $q_{\max} = 8.6 \times 10^{-3}$  Å<sup>-1</sup> due to the liquid-like positional short-range order of the nanorods in the plane perpendicular to the director.

The various dispersion relations are shown in Figure 3. The relaxation rate in the nematic phase, perpendicular to the director ( $N, \perp$ , solid triangles) is linear in  $q_\perp^2$ , roughly up to the position of the structure peak. At higher  $q_\perp$ , the slope increases abruptly, before approaching a final linear regime. In contrast, the behaviour along the director ( $N, \parallel$ , open diamonds) is linear over the accessible range, which is limited by the rapid fall-off of the intensity in this direction (see Figure 1a). In the isotropic phase (with  $\phi_g = 2\%$ ), the dispersion relation is also linear over the entire range.

Let us define the collective diffusion coefficient  $D_{N,\perp}(q_\perp) = \Gamma(q_\perp)/q_\perp^2$ , shown in Figure 4b). For ref-

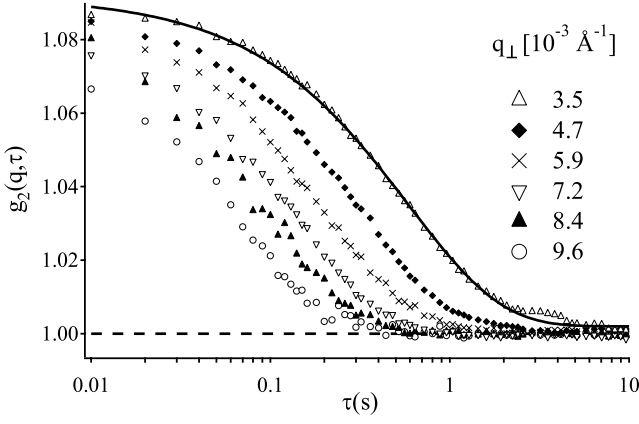


FIG. 2. Autocorrelation functions for a nematic sample with  $\phi_g = 6.7\%$  at different scattering vectors  $q_\perp$ . The solid line is the fit with a stretched exponential (the stretching exponent is about 0.6 for all the curves).

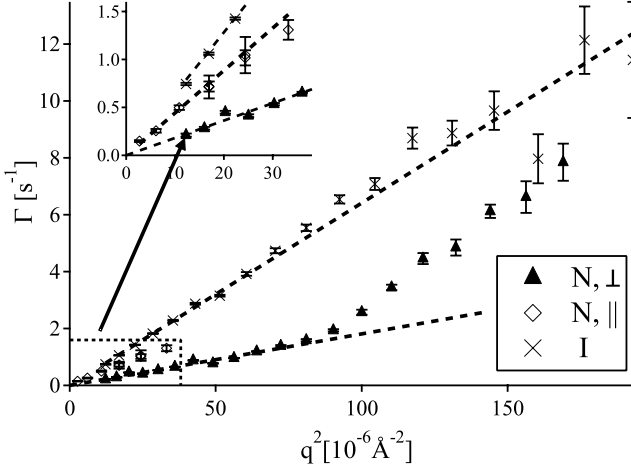


FIG. 3. Dispersion relations for a nematic ( $\phi_g = 6.7\%$ ) sample, with  $\vec{q}$  parallel to the nematic director ( $\diamond$ ), and with  $\vec{q}$  perpendicular to the nematic director ( $\blacktriangle$ ). The dispersion relation of an isotropic, ( $\phi_g = 2\%$ ) sample is shown for comparison ( $\times$ ).

erence, panel a) shows the structure factor (Figure 1b).

Two regimes (above and below the interaction peak of the structure factor) can be clearly distinguished. Between them, the diffusion coefficient jumps by more than a factor of 3. To quantify this variation, we fit  $D_{N,\perp}(q_\perp)$  with a sigmoidal function (solid line in Figure 4b):

$$D(q) = D_{\min} + \frac{D_{\max} - D_{\min}}{1 + \exp\left(-\frac{q - q_{1/2}}{\Delta q}\right)} \quad (1)$$

with parameters:  $D_{\min} = 1.1 \times 10^{-16}$  and  $D_{\max} = 3.4 \times 10^{-16} \text{ m}^2/\text{s}$  while  $q_{1/2} = 9.6 \times 10^{-3}$  and  $\Delta q = 0.45 \times 10^{-3} \text{ \AA}^{-1}$ . The greyed areas around the fit are the  $\pm\sigma$  prediction bands, quantifying the data scatter (about 68 % of the experimental points should fall within this area). The fit function (1) is only chosen for convenience;

there is no physical reason for adopting it.

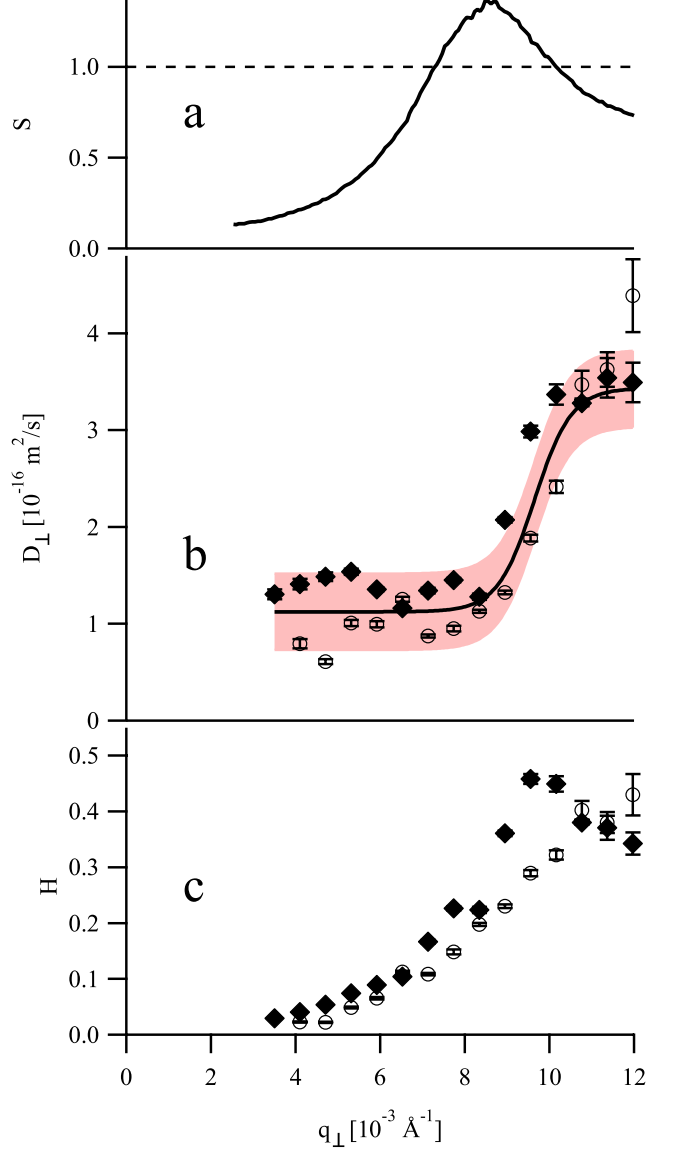


FIG. 4. a) Static structure factor  $S(q_\perp)$ . b) Diffusion coefficient  $D_{N,\perp}(q_\perp)$ . The symbols correspond to two different measurements performed on the same sample. The solid line and the greyed area are the fit by a sigmoidal function and the  $\pm\sigma$  prediction bands (see text). c) Hydrodynamic function obtained using Equation 2. The data are plotted against a common  $q_\perp$  axis.

The decrease of  $D_{N,\perp}(q_\perp)$  at low wave vectors is even more striking if we recall that, for  $q_\perp$  vectors below the peak, where the structure factor decreases, the diffusion coefficient should *increase*! We can restate this result more precisely in terms of the *hydrodynamic function*,  $H(q_\perp)$ , defined by<sup>18</sup>:

$$H(q_\perp) = \frac{D_{N,\perp}(q_\perp)}{D_{0,\perp}} S(q_\perp) \quad (2)$$

and shown in Figure 4c).

Care must be exercised when determining the constant factor  $D_{0,\perp}$ , which is the diffusion coefficient of the particles at infinite dilution. The  $\perp$  subscript specifies that one should consider the diffusion in the direction perpendicular to the main axis of the particle (in the nematic phase this axis is parallel to the director, and we are now concerned with diffusion perpendicular to the director). We start by measuring the (orientationally averaged) diffusion coefficient in the isotropic phase,  $D_I$ . For  $\phi_g = 2\%$ , the data is shown in Figure 3 (crosses), along with a linear fit yielding  $D_I(2\%) = 6.4 \times 10^{-16} \text{ m}^2 \text{ s}^{-1}$ . Similar measurements at  $\phi_g = 0.5\%$  (data not shown) give  $D_I(0.5\%) = 8.0 \times 10^{-16} \text{ m}^2 \text{ s}^{-1}$ . Correcting these results for the intrinsic viscosity of nanorod suspensions<sup>19</sup> leads to an infinite dilution value  $D_0 = D_I(0) = 8.5 \times 10^{-16} \text{ m}^2 \text{ s}^{-1}$ . In isotropic solution,  $D_0$  is a geometric combination of the diffusion coefficients along and perpendicular to the major axis:  $3D_0 = D_{0,\parallel} + 2D_{0,\perp}$  and, for nanorods with an aspect ratio of 10,  $D_{0,\perp}/D_0 = 0.88$ <sup>20</sup>, resulting in  $D_{0,\perp} = 7.5 \times 10^{-16} \text{ m}^2 \text{ s}^{-1}$ .

At high  $q_\perp$ ,  $H(q)$  reaches a value lower than one ( $H(\infty) \simeq 0.4$ ). For spherical particles, this limit is described by<sup>21</sup>:  $H(\infty) = \eta_0/\eta$ , where  $\eta$  is the viscosity of the suspension and  $\eta_0$  that of the solvent. Transposing this formula to our (non-spherical) system yields fairly good agreement<sup>22</sup>. The main feature of  $H(q)$  is however the decrease at lower wave vector, starting around  $q_{\text{max}}$  and clearly visible in Figure 4c). At the lowest accessible wave vector  $H(q) \simeq 0.04$ , ten times smaller than the maximum value  $H(\infty)$ .

Hydrodynamic slowing down of the collective relaxation is also encountered in suspensions of spherical particles, but its amplitude is much lower; for a volume fraction  $\phi = 9\%$  (higher than in our nematic phase),  $H(0)/H(\infty) \simeq 1/3$ <sup>11</sup>. Experimental and theoretical results for even higher volume fractions of spheres (both in the low- and high-salt concentration regimes) yield more modest decreases for the collective diffusion<sup>23</sup>. We conclude that the behaviour of  $H(q)$  at low wave vectors in the nematic phase is very different from that in sphere suspensions.

A possible explanation for this difference is that, if the major axis of the particles is much longer than the typical distance between them, (in the limit of very large order parameter and aspect ratio) the nematic phase should behave like a two-dimensional (2D) system<sup>24</sup>, where hydrodynamic interactions are stronger than for a three-dimensional system<sup>25</sup>. This explanation is in qualitative agreement with recent simulations of 2D colloidal suspensions, where the hydrodynamic interactions slow down the collective diffusion coefficient<sup>26</sup>. In particular, for the volume fraction used in our study these authors find that the hydrodynamic interactions slow down the collective diffusion by at least a factor of four (Ref. 26, Figure 2b). However, more theoretical or numerical results would be needed, in particular concerning the length-scale dependence of the diffusion coefficient  $D(q)$ , to understand this pronounced slowing down.

## ACKNOWLEDGMENTS

A.S.Poulos gratefully acknowledges support from a Marie Curie action (MEST-CT-2004-514307) and from a Triangle de la Physique contract (OTP 26784).

- <sup>1</sup>P. C. Martin, O. Parodi, and P. S. Pershan, *Physical Review A* **6**, 2401 (1972).
- <sup>2</sup>Orsay Liquid Crystal Group, *Physical Review Letters* **22**, 1361 (1969).
- <sup>3</sup>M. J. Stephen and J. P. Straley, *Rev. Mod. Phys.* **46**, 617 (1974).
- <sup>4</sup>T. Kirchhoff, H. Löwen, and R. Klein, *Physical Review E* **53**, 5011 (1996).
- <sup>5</sup>P. P. Jose and B. Bagchi, *J. Chem. Phys.* **125**, 184901 (2006).
- <sup>6</sup>R. Bandyopadhyay, D. Liang, H. Yardimci, D. A. Sessoms, M. A. Borthwick, S. G. J. Mochrie, J. L. Harden, and R. L. Leheny, *Physical Review Letters* **93**, 228302 (2004).
- <sup>7</sup>A. Madsen, J. Als-Nielsen, and G. Grübel, *Physical Review Letters* **90**, 085701 (2003).
- <sup>8</sup>P. N. Pusey, in *Liquids, Freezing and the Glass Transition* (North-Holland, Amsterdam, 1991) pp. 763–942, section 5.2.
- <sup>9</sup>P. G. de Gennes, *Physica* **25**, 825 (1959).
- <sup>10</sup>C. Graf, M. Deggelmann, M. Hagenbüchle, H. Kramer, R. Krause, C. Martin, and R. Weber, *J. Chem. Phys.* **95**, 6284 (1991).
- <sup>11</sup>A. Robert, J. Wagner, W. Härtl, T. Autenrieth, and G. Grübel, *The European Physical Journal E-Soft Matter* **25**, 77 (2008).
- <sup>12</sup>D. M. E. Thies-Weesie, J. P. de Hoog, M. H. H. Mendiola, A. V. Petukhov, and G. J. Vroege, *Chem. Mater.* **19**, 5538 (2007).
- <sup>13</sup>B. J. Lemaire, P. Davidson, J. Ferré, J. P. Jamet, D. Petermann, P. Panine, I. Dozov, and J. P. Jolivet, *The European Physical Journal E-Soft Matter* **13**, 291 (2004).
- <sup>14</sup>G. J. Vroege and H. N. W. Lekkerkerker, *Reports on Progress in Physics* **55**, 1241 (1992).
- <sup>15</sup>B. J. Lemaire, P. Davidson, D. Petermann, P. Panine, I. Dozov, D. Stoensescu, and J. P. Jolivet, *The European Physical Journal E-Soft Matter* **13**, 309 (2004).
- <sup>16</sup>B. J. Lemaire, P. Davidson, J. Ferré, J. P. Jamet, P. Panine, I. Dozov, and J. P. Jolivet, *Physical Review Letters* **88**, 125507 (2002).
- <sup>17</sup>A. Fluerasu, A. Moussaïd, A. Madsen, and A. Schofield, *Physical Review E* **76**, 010401(R) (2007).
- <sup>18</sup>G. Nägele and P. Baur, *Physica A* **245**, 297 (1997).
- <sup>19</sup>M. J. Solomon and D. V. Boger, *Journal of Rheology* **42**, 929 (1998).
- <sup>20</sup>M. M. Tirado, C. L. Martinez, and J. G. de la Torre, *The Journal of Chemical Physics* **81**, 2047 (1984).
- <sup>21</sup>C. W. J. Beenakker and P. Mazur, *Physica A* **120**, 388 (1984).
- <sup>22</sup>Considering an ionic strength of 10 mM, the data of Solomon and Boger<sup>19</sup> give a value of  $\eta_0/\eta = 0.41$  using the low concentration expansion and 0.25 using the overall formula (for an aspect ratio of 8.4). Rheology measurements performed at room temperature in aqueous suspension at the same concentration (6.7 %) also yield  $\eta_0/\eta = 0.25$ , but the comparison is not straightforward due to the lack of information on the electrostatic effects in the presence of propane-1,3-diol.
- <sup>23</sup>A. J. Banchio, J. Gapinski, A. Patkowski, W. Häußler, A. Fluerasu, S. Sacanna, P. Holmqvist, G. Meier, M. P. Lettinga, and G. Nägele, *Physical Review Letters* **96**, 138303 (2006).
- <sup>24</sup>We define a 2D system as invariant under translation along the normal direction, in contrast with the extensively studied quasi-2D systems that consist of particles confined at an interface or between rigid boundaries.
- <sup>25</sup>J. Happel and H. Brenner, *Low Reynolds number hydrodynamics* (Martinus Nijhoff, 1983).
- <sup>26</sup>E. Falck, J. M. Lahtinen, I. Vattulainen, and T. Ala-Nissila, *The European Physical Journal E-Soft Matter* **13**, 267 (2004).